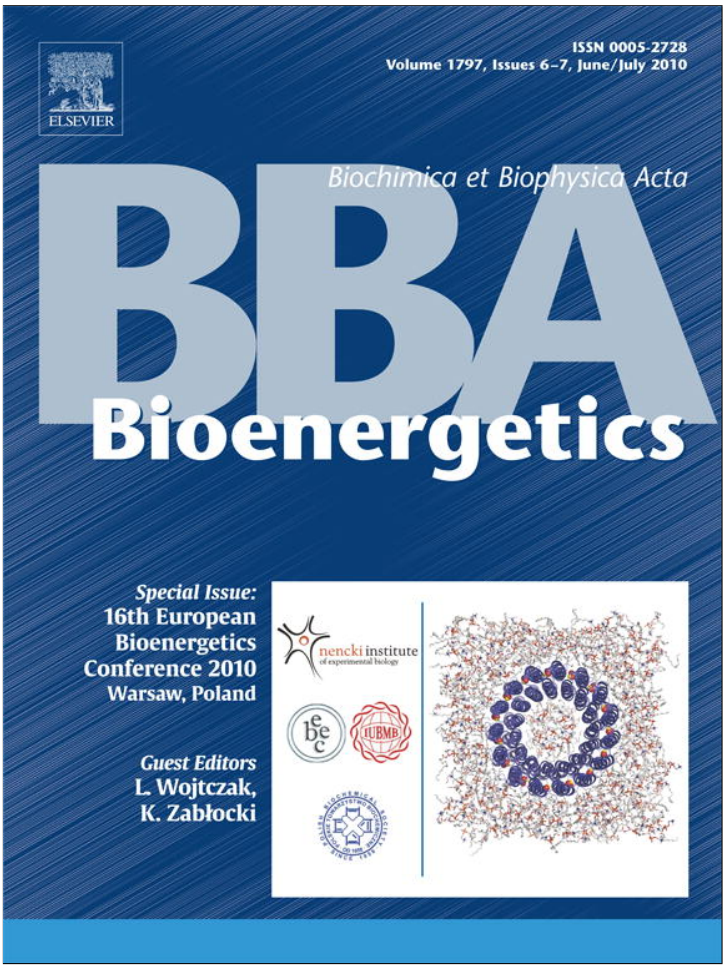

Biochimica et Biophysica Acta 1797 (2010) 664–670

Contents lists available at ScienceDirect

Biochimica et Biophysica Acta

journal homepage: www.elsevier.com/locate/bbabio

Review

Structure and function of mitochondrial supercomplexes

Natalya V. Dudkina [a], Roman Kouřil [a], Katrin Peters [b], Hans-Peter Braun [b], Egbert J. Boekema [a,*]

[a] Electron microscopy group, Groningen Biomolecular Sciences and Biotechnology Institute, University of Groningen, Nijenborgh 4, 9747 AG Groningen, The Netherlands
[b] Institute for Plant Genetics, Faculty of Natural Sciences, Universität Hannover, Herrenhäuser Str. 2, D-30419 Hannover, Germany

ARTICLE INFO

Article history:
Received 27 October 2009
Received in revised form 14 December 2009
Accepted 16 December 2009
Available online 28 December 2009

Keywords:
Oxidative phosphorylation
Mitochondria
Respirasome
ATP synthase
Electron microscopy
Supercomplex

ABSTRACT

The five complexes (complexes I–V) of the oxidative phosphorylation (OXPHOS) system of mitochondria can be extracted in the form of active supercomplexes. Single-particle electron microscopy has provided 2D and 3D data describing the interaction between complexes I and III, among I, III and IV and in a dimeric form of complex V, between two ATP synthase monomers. The stable interactions are called supercomplexes which also form higher-ordered oligomers. Cryo-electron tomography provides new insights on how these supercomplexes are arranged within intact mitochondria. The structure and function of OXPHOS supercomplexes are discussed.

1. Introduction

Mitochondria are intracellular organelles which accommodate in their inner or cristae membrane large numbers of five oxidative phosphorylation complexes (complexes I–V). The complexes I to IV are oxidoreductases which, with the exception of complex II, couple electron transport with translocation of protons across the inner mitochondrial membrane (Fig. 1). The generated proton motive force is used by ATP synthase (complex V) for ATP synthesis from ADP and phosphate. Complex I or NADH dehydrogenase is the first and major entrance point of electrons to the respiratory chain. It transfers electrons from NADH molecules to a lipophilic quinone designated ubiquinone. Complex II or succinate dehydrogenase transmits electrons from succinate to ubiquinone and directly connects the citric acid cycle to the respiratory chain. From the reduced ubiquinone electrons can be transferred to complex III or cytochrome *c* reductase which exists in the membrane as a functional dimer. The small protein cytochrome *c* mediates electron transfer from cytochrome *c* reductase to cytochrome *c* oxidase (complex IV). Finally, electrons are transferred to molecular oxygen which is reduced to water.

The ideas about the overall organization of these five complexes, which together form the oxidative phosphorylation (OXPHOS) system, have been changing with time. A so-called "fluid-state model" is supported by the finding that all individual protein complexes of the OXPHOS system can be purified to homogeneity in an enzymatically active form and by lipid dilution experiments (reviewed in [1,2]). It postulates that the respiratory chain complexes freely diffuse in membrane and that the electron transfer is based on random collisions of the single complexes.

The fluid-state model is challenged by a "solid-state model" which proposes stable interactions between the OXPHOS complexes within entities named supercomplexes. This model is now supported by a wide range of experimental findings: 1. Supercomplexes can be resolved by blue native polyacrylamide gel electrophoresis (BN-PAGE) [3,4]. 2. Supercomplexes are active as shown by in-gel activity measurements within blue native gels [3,5]. 3. Electron microscopy (EM) structures revealed defined interactions of OXPHOS complexes within the isolated respiratory supercomplexes [6–10]. 4. Flux control experiments [11,12] confirm that the respiratory chain operates as one functional unit. 5. Point mutations in genes encoding one of the subunits of one OXPHOS complex affect the stability of another complex. Thus, complex III is required to maintain complex I in mouse and human cultured cells mitochondria [13]. Complex IV is necessary for the assembly or stability of complex I in mouse fibroblasts [14]. 6. Oxygen uptake by isolated mitochondria of potato correlates with the abundance of supercomplexes [5]. 7. Some supercomplexes need cardiolipin for their formation [15,16]. Until some years ago, the fluid-state model was widely accepted in the field of bioenergetics. The newest edition of the Lehninger textbook is the first general textbook that presents a section on OXPHOS supercomplexes [17].

In many organisms the complexes I, III and IV were found to associate into specific supercomplexes (reviewed in [18]). Only complex II seems not to form part of any respiratory chain supercomplexes. The possible explanation for the singular state of complex II is that it is also involved in the citric acid cycle. However, a recent publication on the OXPHOS system of mouse mitochondria also

* Corresponding author.
E-mail address: e.j.boekema@rug.nl (E.J. Boekema).

0005-2728/$ – see front matter © 2009 Elsevier B.V. All rights reserved.
doi:10.1016/j.bbabio.2009.12.013

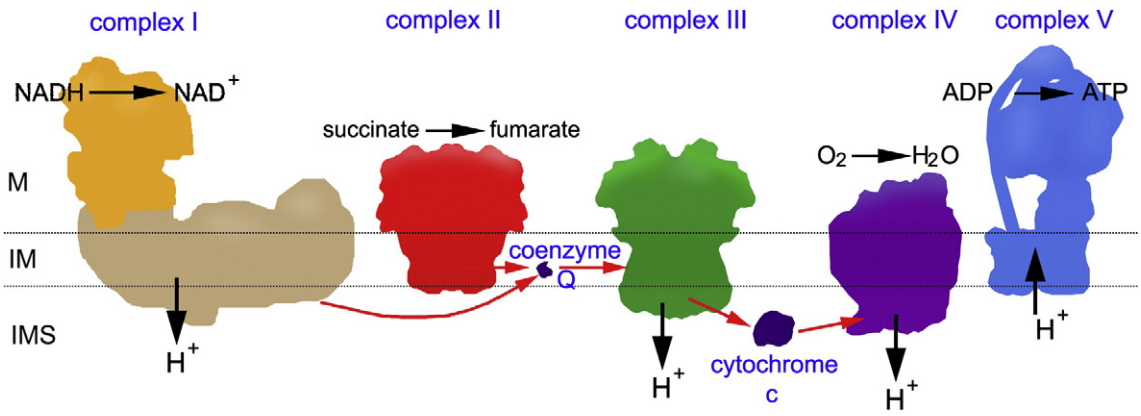

Fig. 1. A schematic representation of the OXPHOS system showing its individual components but ignoring their structural interactions. Note that complex I is depicted here almost as large as complex V. Actually, mammalian complex I is protruding as far as complex V from the membrane, but plant mitochondrial complex I is a bit smaller in size. Complex III is a functional dimer, in contrast to complex IV, although a high-resolution dimeric structure of the latter has been solved by X-ray crystallography. A full picture needs the input of the yet unsolved high-resolution structure of complex I. The position of the matrix (M), the intermembrane space (IMS) and cristae or inner membrane (IM) has been indicated.

reported detection of complex II containing supercomplexes by BN-PAGE [19]. The $I+III_2+IV_{1-2}$ supercomplex is called respirasome because it can autonomously carry out respiration in the presence of ubiquinone and cytochrome *c*. Respiratory supercomplexes are believed to co-exist in the membrane with single OXPHOS complexes. In this review we discuss the structure and function of the various types of supercomplexes within the mitochondrial membrane. In a few cases it appears that supercomplexes further organize into larger structures called *strings*. The clearest example is the ATP synthase complex (complex V), which assembles into long oligomeric chains [20–23].

2. Respiratory supercomplexes

High-resolution crystal structures are available for most OXPHOS complexes [24]. Only complex I, which by far is the largest complex of the respiratory chain, has not been crystallized up to now. It has an unique L-like shape which results from the orthogonal association of its two arms, the matrix-exposed "peripheral arm" and the so-called "membrane arm" [25,26]. However, the overall shape varies in different organisms as revealed by electron microscopy. For instance, plant complex I has a second matrix-exposed domain which is attached to the membrane arm at a central position and which includes carbonic anhydrases [27–29]. Furthermore, complex I of *Yarrowia lipolytica* has an unknown protrusion at the tip of the membrane arm of complex I [26] and complex I from beef an additional density at the membrane arm tip on its matrix-exposed side [18]. The structure of the peripheral arm of complex I from the archaebacterium *Thermus thermophilus* was recently resolved by X-ray crystallography. Positions of eight subunits and all redox centers of the enzyme were determined, including nine iron sulphur centers [30]. There is much less known about the membrane arm. The main known function of the hydrophobic part is proton translocation [31], but the precise functions of the membrane domain and the coupling mechanism are not yet solved because of lack of high-resolution structural data. However, the projection map at 8 Å resolution of complex I from *E. coli* obtained by electron microscopy [32] indicates the presence of about 60 transmembrane α-helices within one membrane domain. A binding site and access channel for quinone is predicted to be at the interface with the peripheral arm. The location of subunits NuoL and NuoM at substantial distance from the peripheral arm, which contains all the redox centers of the complex, indicates that conformational changes likely play a role in the mechanism of coupling between electron transfer and proton pumping.

Complex I can form a stable association with the complex III dimer of the respiratory chain [3,4]. An investigation by single-particle EM revealed the lateral association of dimeric complex III with the tip of the membrane part of complex I in *Arabidopsis* [6], *Zea mays* [28]; see Fig. 2E) and potato [29]. The top-view projection maps of this plant supercomplex all are similar, although in potato it appears that the angle between complex I and III is variable [32]. In the bovine $I+III_2$ supercomplex the association of the complexes I and III_2 is about the same (Fig. 2F), but particles in the top-view position are extremely rare, in contrast to the side views (Fig. 2B).

Complex III_2 can associate with one or up to four copies of complex IV as it was described for potato [33], spinach [34], *Asparagus* [35] and beef [3]. The first detailed structure of a mitochondrial supercomplex was obtained for the III_2+IV_{1-2} supercomplex of *Saccharomyces cerevisiae* [10]. It could be determined because of its high stability in yeast and for the reason that this organism lacks complex I, which can associate to complex III as well, as described above. The supercomplex appeared in different positions and this allowed generating a pseudo-atomic 3D model which shows that monomeric cytochrome *c* oxidase complexes are attached to dimeric complex III at two alternate sides with their convex sides facing the complex III_2. This is the opposite to the side involved in the formation of complex IV dimers as described by X-ray crystallography. Association of the complexes III and IV depends on the presence of cardiolipin within the inner mitochondrial membrane [15,16]. In bovine mitochondria complex I (Fig. 2A) binds to complexes III_2 and IV [18]. These supercomplexes represent the largest form of OXPHOS units and are also termed "respirasomes" [3]. Complex III_2 attaches to the complex I at its membrane arm in a region from middle to tip (Fig. 2B) in a similar way like previously described for the $I+III_2$ supercomplex of *Arabidopsis* [6]. Bovine complex IV seems to be attached to the tip of complex I (Fig. 2C).

To get a closer look to the composition of the respirasome we produced 2D cryo-EM data on the isolated bovine $I+III_2+IV$ supercomplex on carbon support films (Fig. 2I). In contrast to negative stain freezing in an amorphous ice layer preserves the protein in native water-like environment and does not introduce any artifacts which can occur during chemical fixation with salts of heavy metals followed by air-drying. Additionally, cryo-EM allows to see internal details of the object whereas the negative stain reflects only a contour. Remarkably, freezing of the bovine respirasome provoked slightly different orientation of the complex on the carbon support film. The newly obtained projection map at 24 Å resolution (Fig. 2I) resembles the 2D negatively stained projection map of $I+III_2$ supercomplex from *Arabidopsis* and *Zea mays* (Fig. 2E). A low resolution 3D model of complex I [26] together with the crystal structures available for complexes III and IV are useful to understand

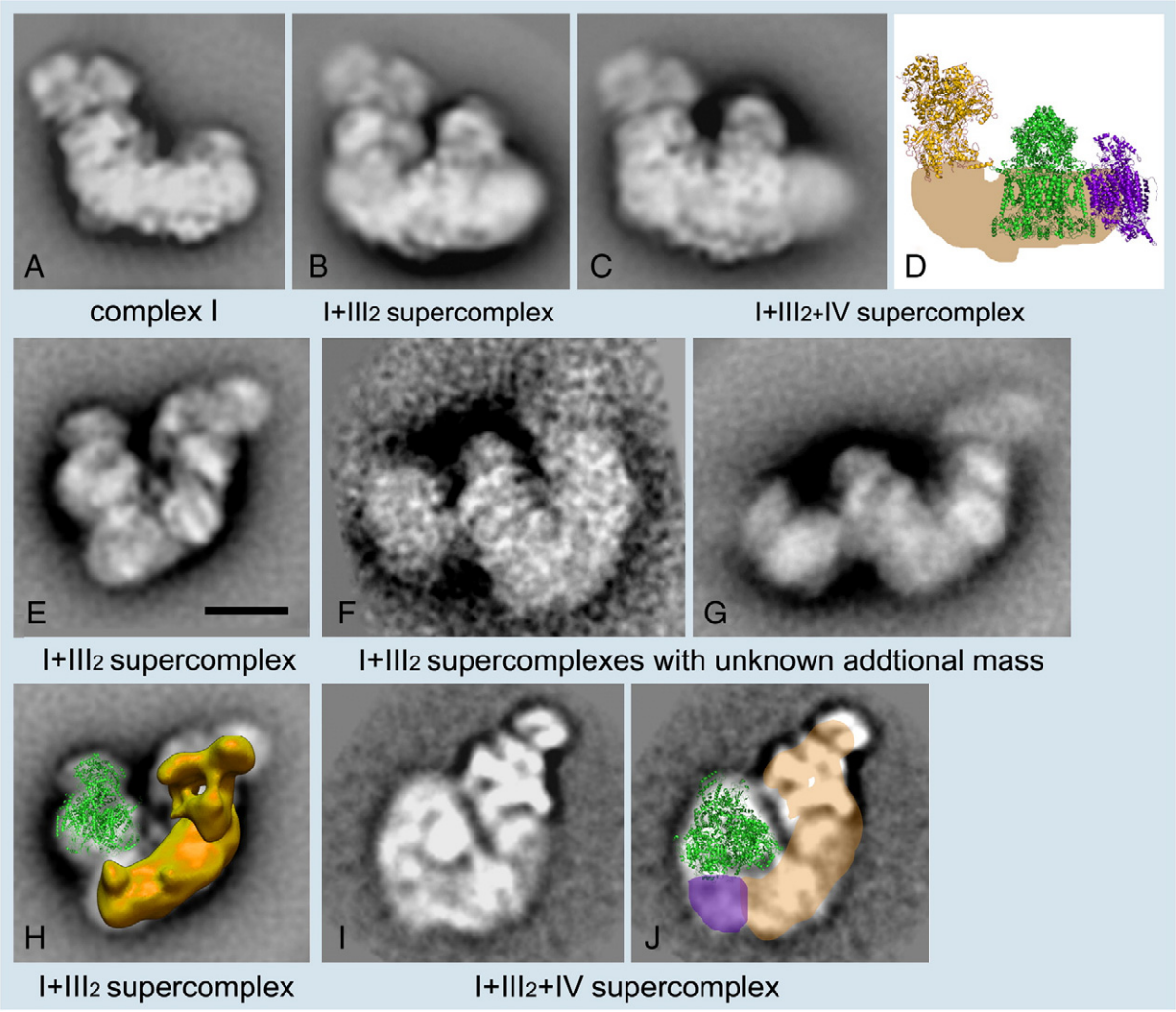

Fig. 2. Examples of EM projection maps of OXPHOS supercomplexes obtained by negative staining (A, B, C, E, F, G, H) and cryo-EM (I, J) plus modelling. (A–C) Averaged side views of bovine complex I and its supercomplexes. (D) Positions of individual complexes within the $I+III_2+IV$ supercomplex or respirasome from bovine mitochondria [18]. Yellow: X-ray structure of the hydrophilic domain of complex I from *Thermus thermophilus* [30], green: dimeric bovine cytochrome *c* reductase (complex III) [52], purple: bovine cytochrome *c* oxidase (complex IV) [53]. (E) Top-view of the $I+III_2$ supercomplex from maize [28]. (F, G) Top-views of $I+III_2$ supercomplexes with an unknown additional mass from bovine and potato mitochondria, respectively (N.V. Dudkina, R. Kouřil, J.B. Bultema, E.J. Boekema, unpublished data). (H) Assignment of the complexes I and III_2 within the top-view map of $I+III_2$ supercomplex from maize, as presented in image (E); the complex III dimer is in green in a tilted position; in yellow the 3D EM structure of complex I from *Yarrowia lipolytica* [26]. (I) Map of the bovine respirasome (N.V. Dudkina, unpublished data). (J) Modelling of the respirasome. In beige the position of the membrane arm of complex I, in green X-ray structure of the bovine dimeric complex III and in purple the position of a complex IV monomer. Scale bar, 10 nm.

the respirasome architecture. We can precisely assign the positions of complexes III_2 (Fig. 2J, in green) and I (Fig. 2J, in yellow) within the revealed structure and deduce the same overall association of complexes I and III_2 as in the plant supercomplex (Fig. 2H). The small additional density at the tip of complex I and next to the complex III_2 should represent a complex IV monomer. The rotational orientation of complex IV remains unclear and requires further investigation.

Both the 3D model of complex I [26] and the 2D cryo-EM projection map of the membrane arm of complex I [32] clearly show the curved shape of the membrane-embedded part of complex I. Our 2D projection data of *Arabidopsis*, potato, maize and bovine complex I show the same structural feature. Importantly, the curved feature of the membrane arm can be used as an indicator for a handedness determination of 3D models. Here we can apologize for a wrong handedness in Dudkina et al. [6], as at that time these data were not available. Because it now appears that there is no difference between the bovine and plant $I+III_2$ supercomplex, we conclude that complex III is always attached to complex I at its inner curved side. This is contradictory to the proposed 3D model at 32 Å resolution in negative stain of the bovine respirasome [36], where complex III is attached at the outside part of the complex I. Evidently, the 3D density map was not correctly assigned. A closer look to their 3D model viewed from the inner membrane side (IMS) clearly shows the typical curvature of the membrane part of complex I, which was omitted in the assignment of the respirasome.

3. Higher organization levels of respiratory supercomplexes

It now appears that the supercomplex formation is not the highest level of OXPHOS organization. A row-like organization of OXPHOS complexes I, III and IV into respiratory strings has been proposed, based on biochemical evidence. It was suggested that respirasomes are interconnected with III_2+IV_4 supercomplexes [37]. However, it appears that such transient strings cannot be purified after detergent solubilization which limits structural studies. Hence, the proposed respiratory string was approached by an extensive structural characterization of all its possible breakdown products, which are the various types of supercomplexes. About 400,000 molecular projections of supercomplexes from potato mitochondria were processed

by single-particle electron microscopy [29]. Two-dimensional projection maps of at least five different supercomplexes, including $I+III_2$, III_2+IV_1, V_2, $I+III_2+IV_1$ and I_2+III_2 supercomplexes in different types of position, were obtained. From these maps the relative position of the individual complexes in the largest unit, the $I_2+III_2+IV_2$ supercomplex, could be determined in a coherent way. The maps also show that the $I+III_2+IV_1$ supercomplex, or respirasome, differs from its counterpart in bovine mitochondria. The new structural features allow us to propose a consistent model of the respiratory string for bovine and potato mitochondria, composed of repeating $I_2+III_2+IV_2$ units (Fig. 3, [29]), which is in agreement with dimensions observed in former freeze-fracture electron microscopy data [23]. This model modifies and extends the hypothetical scheme presented in [37]. There is, however, some evidence for other types of interactions occurring at low frequencies. We found by classification of all breakdown products from cristae membranes big particles, composed of a $I+III_2$ supercomplex plus a large additional mass in bovine (Fig. 2F) and potato membranes (Fig. 2G), (N.V. Dudkina, R. Kouřil, J.B. Bultema, E.J. Boekema, unpublished data). The composition of the additional mass is unknown, but it appears to be larger than a single copy of complex IV, because these novel particles are larger than the respirasome (Fig. 2I, J).

Another example of a higher-level organization of supercomplexes, dealing with oligomeric ATP synthase, is discussed in the next section.

4. The dimeric ATP synthase supercomplex and its oligomeric organization

Mitochondrial F_1F_0 ATP synthase is a complex of 600 kDa formed by 15–18 subunits [38,39]. The matrix-exposed water soluble F_1 part is constituted of three α and three ß subunits and connected to the membrane-embedded ring-like F_0 part via central and peripheral stalks. The F_0-part is composed of subunits a (Su 6), A6L (Su 8), e, f, g, the central stalk consists of the γ, δ and ε subunits and the peripheral stalk is made from subunits OSCP (Su 5), b, d, F6 (h) (different names of the yeast counterparts in brackets, reviewed in [40]). The yeast protein has two additional, specific subunits i and k. A monomer is active in ATP catalysis and hydrolysis like its counterpart in prokaryotes, but evidence for a dimeric organization of the ATP synthase complex came as a surprise from BN-PAGE work on yeast [41]. The 1200 kDa dimeric complex includes dimer specific subunits e, g and k, which were not detected in monomers. Later, dimers were found in beef, *Arabidopsis* and several other organisms [3,4]. The dimer specific subunits e and g, as well as the subunits a, b, h and i of the monomer, stabilize the monomer–monomer interface [40]. To date, 2D maps of dimeric ATP synthase are available for bovine [8], the colorless green alga *Polytomella* [7] and *S. cerevisiae* [21] obtained by single-particle electron microscopy. In all organisms two monomers associate via the membrane F_0 parts and make an angle, which can be fixed or variable between 35 and 90°. Dimeric ATP synthase from *Polytomella* seems to be the most stable one and the monomers make one specific angle of 70°, as discussed below (Fig. 4C).

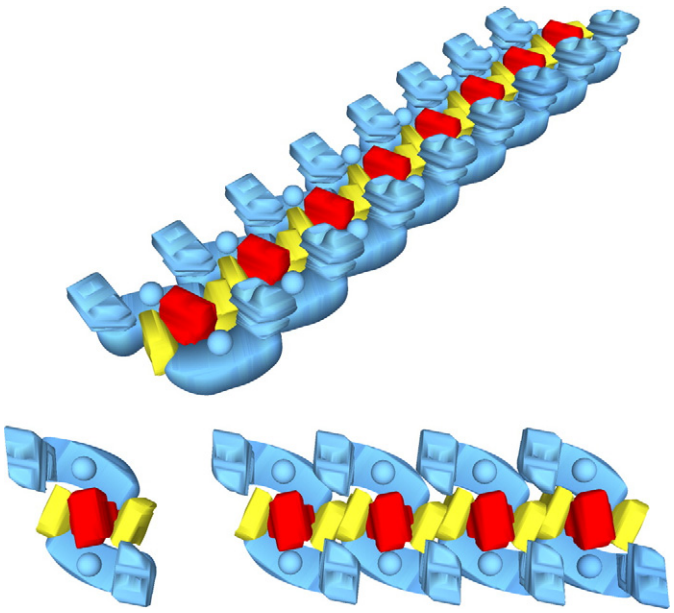

Fig. 3. A schematic model of the organization of respiratory chain complexes into a respiratory string. The basic unit (lower left) consists of two copies of complex I (blue), one copy of complex III_2 (red), and two copies of complex IV (yellow). Association of basic units into a string is mediated by complex IV, which interacts with a neighbouring complex IV through a dimeric interface found in the X-ray structure [52]; (from [29], modified).

Despite the fact that the ATP synthase dimers were first described in the 1990s [41], older work even hint at a higher type of organization as oligomers. Rows of dimeric ATP synthases were demonstrated in *Paramecium* mitochondria by rapid-freeze deep-etch electron microscopy [23]. Additional BN-PAGE evidence of trimeric and tetrameric organizations of mammalian ATP synthases [20] supports the hypothesis of an oligomeric arrangement of ATP synthases in the membrane. Another BN-PAGE work on mammalian enzyme revealed only ATP synthase fragments with an even number of ATP synthases [42]. Ultrasectioning and negative staining of osmotically shocked *Polytomella* mitochondria came to the same conclusion [21]. Later, atomic force microscopy on isolated inner membranes from baker's yeast revealed rows of dimeric ATP synthases, although remarkably no curvature of the membrane was shown at all, likely due to flattening of the membrane on the substrate [43]. This is in contrast with the fact that isolated bakers' yeast ATP synthase dimers make a large angle [21]. Recently cryo-electron tomography (cryo-ET) data on bovine and rat fragmented mitochondria demonstrated long rows of dimers located at locally curved cristae membranes [22]. Averaging also revealed larger angles between monomers than reported for isolated bovine dimeric ATP synthase [8]. In another study, dimeric ATP synthase was studied in intact *Polytomella* mitochondria. Cryo-ET experiments with mitochondria embedded in amorphous ice showed the presence of oligomeric rows of ATP synthases in mitochondrial cristae [44]. Details of the rows were obtained at a resolution of 5.7 nm by averaging subvolumes of tomograms; this shows that the oligomeric chain is composed of repeating dimeric units with a spacing of 12 nm. The monomers make contact via the membrane part and the peripheral stalk (Fig. 4B) and individual dimers resemble very well the projection maps of isolated dimers in negative stain (Fig. 4C) [7] and amorphous ice (Fig. 4E) as can be seen from the connection of the stator to the F_1 headpiece (yellow arrows). The dimer–dimer interface is not yet well understood. The resolution of 5.7 nm for *Polytomella* appears in the same range as the 5 nm resolution claimed for the ATP synthase oligomers from bovine and rat liver dimers [22]. However, in contrast to the *Polytomella* data, the F_1 headpieces in the latter work merely look like feature-less spheres. In conclusion, the tomography data convincingly show the oligomeric state of the ATP synthase complex, but are far too low in resolution to reveal subunit interactions. From biochemical experiments it was predicted that subunits e, f, g, Su 8 (A6L), some transmembrane helixes of the a-subunit as well as carriers for inorganic phosphate and for ADP/ATP are potential candidates for the oligomerization of ATP synthases [40].

5. Potential functions of OXPHOS supercomplexes

The occurrence of several specific supercomplexes and higher-ordered oligomers must have functional reasons. It was proposed that OXPHOS supercomplexes allow enhancement of the flow of electrons

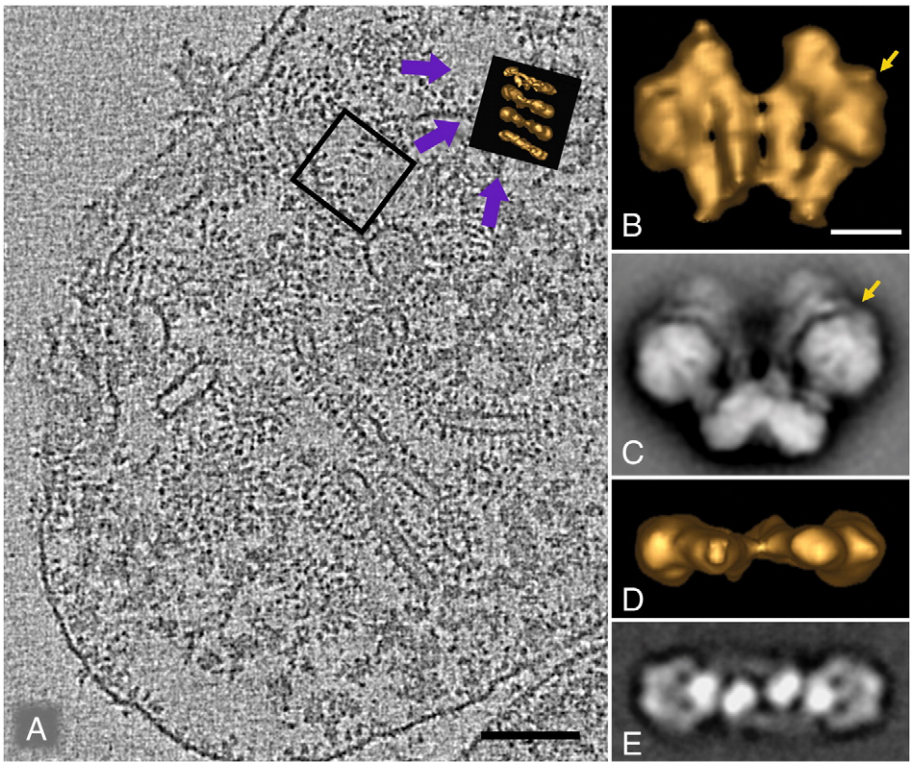

Fig. 4. Electron tomography of *Polytomella* mitochondria reveals the arrangement of oligomeric ATP synthase molecules. (A) Section of a tomogram (3D reconstruction) calculated from dual-axis electron tomography of an ice-embedded mitochondrion [44]. To reveal fine detail, hundreds of boxed subvolumes with a size as indicated were selected from several tomograms, as symbolized by purple arrows, aligned and averaged. (B) A single molecule of dimeric ATP synthase from tomography data in a side-view position, selected from the averaged subvolume from image A at a 4× larger scale. (C) Side-view of isolated ATP synthase in negative stain [7]. (D) Top-view of the same dimeric ATP synthase from tomography data as in B. (E) Top-view of isolated ATP synthase calculated by single-particle cryo-EM. Bar scale for frame A, 100 nm. Bar scale for frames B–E, 10 nm. The yellow arrows mark the connection between the F_1 headpiece and the peripheral stalk.

between the complexes by reducing the distance of diffusion of the mobile electron carriers ubiquinone and cytochrome *c* or by substrate channeling between associated OXPHOS complexes [10,45]. A direct role of the $I+III_2(+IV_{1-2})$ supercomplex in ubiquinone-channeling is not clear so far, because the ubiquinone-binding domain of complex I possibly is not in close proximity to the complex I–complex III_2 interphase [6]. However, even if direct channeling does not take place, transfer of ubiquinol from complex I to complex III_2 still might be facilitated due to reduced diffusion distances. In plants the $I+III_2$ supercomplex might be necessary for the regulation of alternative respiration by reducing access of alternative oxidase to ubiquinol [4]. In yeast formation of the III_2+IV_{1-2} supercomplex seems to optimize the electron transport between complexes III and IV by a contraction of the cytochrome *c* movement between these two complexes [10]. The same can be valid for potato mitochondria based on the facts that complexes I, III and IV are rate limiting in flux control experiments and cytochrome *c* was found in the supercomplex [2]. Meantime, the same experiments did not demonstrate this for bovine heart mitochondria. Finally, supercomplex formation was suggested to be important in preventing excess oxygen radical formation [2].

Besides functional reasons, supercomplex formation is necessary for assembly and stability of its individual components. As an example, complex I is necessary for fully assembled complex III in human patients with mutations in the complex I subunits NDUFS2 and NDUFS4 [46] and the absence in complex III results in a dramatic loss of complex I in humans [47]. Furthermore, complex IV is required for the assembly of complex I in fibroblasts [14] and complex III_2 is essential for the stability of complex I in mouse cells [13]. The need for a higher organization in supercomplexes might be a more general requirement because in *Paracoccus denitrificans* assembly of respiratory complexes I, III, and IV into the respirasome stabilizes complex I [48].

The occurrence of ATP synthase dimers and oligomers has a special reason. Dimerization leads to a local curvature of the cristae membrane. Ultrastructural studies on yeast null mutants of dimer specific e and g subunits which lack the dimeric state of ATP synthases indicated that their mitochondria exhibit an unusual onion-shape morphology without any membrane foldings [49,50]. This strongly suggests that dimerization of ATP synthases is essential for cristae morphology. A recent study on mammalian mitochondria proved the organization of ATP synthases in long ribbons of dimers. The mitochondrial cristae may act as proton traps and enhance the local proton gradient necessary for ATP synthesis. In this way ATP synthases may optimize their own performance under proton-limited conditions [22].

6. Prospectives

Up to now a large amount of data on the OXPHOS system has been collected with different biochemical and biophysical techniques. Nevertheless, a complete picture of the protein organization in the cristae membrane is not yet available. Much higher resolution structural data on specific supercomplexes are necessary to give a full interpretation at the atomic level of subunit interactions and electron flow. The structural information of the dimeric ATP synthase complex, $I+III_2$ supercomplex and the respirasome should be improved by either X-ray crystallography or single-particle electron microscopy. The organisms discussed above, such as *Polytomella*, are obvious candidates to provide the most stable types of supercomplexes.

Despite the fact that the oligomeric organization of ATP synthases has now been proven, the position of the other OXPHOS complexes, in particular the respirasomes, within the cristae membrane is still unclear. According to [22], respirasomes and single respiratory complexes could be located in the less curved regions of the cristae membrane. Another

possibility would be a localization between the rows of ATP synthases. However, available data suggest that likely the amount of respiratory chain complexes is very limited in comparison to ATP synthases and it is difficult to detect them at this resolution. A breakthrough is expected by further application of cryo-electron tomography, as discussed for ATP synthase oligomers (Fig. 4). Electron tomography is an emerging technique, but still limited in resolution. In addition to 3D averaging and classification of individual subvolumes improvement in resolution is expected in the near future by perfecting cryo-electron microscopy hardware and software, and implementing the new generation of direct electron detectors, replacing the currently used inefficient slow-scan CCD cameras.

Finally, our understanding of supercomplex organization will also increase by studying the structural aspects of the many naturally occurring mutants of the OXPHOS system. Since the first report of a complex I deficit related to a human mitochondrial disorder in 1988, many other mitochondrial diseases have been associated to structural and functional defects at the level of this enzyme complex I (see for instance [46,51]).

Acknowledgements

We thank Mr. Jelle Bultema for discussion. This work was supported by the Netherlands organization of scientific research (NWO) and by the Deutsche Forschungsgemeinschaft (grant Br 1829-8/1).

References

[1] C.R. Hackenbrock, B. Chazotte, S.S. Gupte, The random collision model and a critical assessment of diffusion and collision in mitochondrial electron transport, J. Bioenerg. Biomembr. 18 (1986) 331–368.
[2] G. Lenaz, M.L. Genova, Structural and functional organization of the mitochondrial respiratory chain: a dynamic super-assembly, Int. J. Biochem. Cell Biol. 41 (2009) 1750–1772.
[3] H. Schägger, K. Pfeiffer, Supercomplexes in the respiratory chains of yeast and mammalian mitochondria, EMBO J. 19 (2000) 1777–1783.
[4] H. Eubel, L. Jänsch, H.-P. Braun, New insights into the respiratory chain of plant mitochondria supercomplexes and a unique compositions of complex II, Plant Physiol. 133 (2003) 274–286.
[5] H. Eubel, J. Heinemeyer, S. Sunderhaus, H.P. Braun, Respiratory chain supercomplexes in plant mitochondria, Plant Physiol. Biochem. 42 (2004) 937–942.
[6] N.V. Dudkina, H. Eubel, W. Keegstra, E.J. Boekema, H.-P. Braun, Structure of a mitochondrial supercomplex formed by respiratory-chain complexes I and III, Proc. Natl. Acad. Sci. USA 102 (2005) 3225–3229.
[7] N.V. Dudkina, J. Heinemeyer, W. Keegstra, E.J. Boekema, H.P. Braun, Structure of dimeric ATP synthase from mitochondria: an angular association of monomers induces the strong curvature of the inner membrane, FEBS Lett. 579 (2005) 5769–5772.
[8] F. Minauro-Sanmiguel, S. Wilkens, J.J. García, Structure of dimeric mitochondrial ATP synthase: novel F_0 bridging features and the structural basis of mitochondrial cristae biogenesis, Proc. Natl. Acad. Sci. USA 102 (2005) 12356–12358.
[9] E. Schäfer, H. Seelert, N.H. Reifschneider, F. Krause, N.A. Dencher, J. Vonck, Architecture of active mammalian respiratory chain supercomplexes, J. Biol. Chem. 281 (2006) 15370–15375.
[10] J. Heinemeyer, H.P. Braun, E.J. Boekema, R. Kouřil, A structural model of the cytochrome *C* reductase/oxidase supercomplex from yeast mitochondria, J. Biol. Chem. 282 (2007) 12240–12248.
[11] H. Boumans, L.A. Grivell, J.A. Berden, The respiratory chain in yeast behaves as a single functional unit, J. Biol. Chem. 273 (1998) 4872–4877.
[12] C. Bianchi, M.L. Genova, G.P. Castelli, G. Lenaz, The mitochondrial respiratory chain is partially organized in a supercomplex assembly: kinetic evidence using flux control analysis, J. Biol. Chem. 279 (2004) 36562–36569.
[13] R. Acín-Pérez, M. Bayona-Bafaluy, P. Fernández-Silva, R. Moreno-Loshuertos, A. Pérez-Martos, C. Bruno, C. Moraes, J. Enríquez, Respiratory complex III is required to maintain complex I in mammalian mitochondria, Mol. Cell 13 (2004) 805–815.
[14] F. Diaz, H. Fukui, S. Garcia, C.T. Moraes, Cytochrome *c* oxidase is required for the assembly/stability of respiratory complex I in mouse fibroblasts, Mol. Cell Biol. 26 (2006) 4872–4881.
[15] M. Zhang, E. Mileykovskaya, W. Dowhan, Gluing the respiratory chain together. Cardiolipin is required for supercomplex formation in the inner mitochondrial membrane, J. Biol. Chem. 277 (2002) 43553–43556.
[16] K. Pfeiffer, V. Gohil, R.A. Stuart, C. Hunte, U. Brandt, M.L. Greenberg, H. Schägger, Cardiolipin stabilizes respiratory chain supercomplexes, J. Biol. Chem. 278 (2003) 52873–52880.
[17] D.L. Nelson, M.M. Cox, Lehninger Principles of Biochemistry, Fifth editionW.H. Freeman, New York, 2008.
[18] N.V. Dudkina, S. Sunderhaus, E.J. Boekema, H.P. Braun, The higher level of organization of the oxidative phosphorylation system: mitochondrial supercomplexes, J. Bioenerg. Biomembr. 40 (2008) 419–424.
[19] R. Acín-Pérez, P. Fernández-Silva, M.L. Peleato, A. Pérez-Martos, J.A. Enriquez, Respiratory active mitochondrial supercomplexes, Mol. Cell 32 (2008) 529–539.
[20] F. Krause, N.H. Reifschneider, S. Goto, N.A. Dencher, Active oligomeric ATP synthases in mammalian mitochondria, Biochem. Biophys. Res. Commun. 329 (2005) 583–590.
[21] N.V. Dudkina, S. Sunderhaus, H.P. Braun, E.J. Boekema, Characterization of dimeric ATP synthase and cristae membrane ultrastructure from *Saccharomyces* and *Polytomella* mitochondria, FEBS Lett. 580 (2006) 3427–3432.
[22] M. Strauss, G. Hofhaus, R.R. Schröder, W. Kühlbrandt, Dimer ribbons of ATP synthase shape the inner mitochondrial membrane, EMBO J. 27 (2008) 1154–1160.
[23] R.D. Allen, C.C. Schroeder, A.K. Fok, An investigation of mitochondrial inner membranes by rapid-freeze deep-etch techniques, J. Cell Biol. 108 (1989) 2233–2240.
[24] P.R. Rich, The molecular machinery of Keilin's respiratory chain, Biochem. Soc. Trans. 31 (2003) 1095–1105.
[25] V. Guenebaut, R. Vincentelli, D. Mills, H. Weiss, K.R. Leonard, Three-dimensional structure of NADH-dehydrogenase from *Neurospora crassa* by electron microscopy and conical tilt reconstruction, J. Mol. Biol. 265 (1997) 409–418.
[26] M. Radermacher, T. Ruiz, T. Clason, S. Benjamin, U. Brandt, V. Zickermann, The three-dimensional structure of complex I from *Yarrowia lipolytica*: a highly dynamic enzyme, J. Struct. Biol. 154 (2006) 269–279.
[27] S. Sunderhaus, N.V. Dudkina, L. Jänsch, J. Klodmann, J. Heinemeyer, M. Perales, E. Zabaleta, E.J. Boekema, H.-P. Braun, Carbonic anhydrase subunits form a matrix-exposed domain attached to the membrane arm of mitochondrial complex I in plants, J. Biol. Chem. 281 (2006) 6482–6488.
[28] K. Peters, N.V. Dudkina, L. Jänsch, H.P. Braun, E.J. Boekema, A structural investigation of complex I and $I+III_2$ supercomplex from *Zea mays* at 11–13 Å resolution: assignment of the carbonic anhydrase domain and evidence for structural heterogeneity within complex I, Biochim. Biophys. Acta 1777 (2008) 84–93.
[29] J.B. Bultema, H.P. Braun, E.J. Boekema, R. Kouřil, Megacomplex organization of the oxidative phosphorylation system by structural analysis of respiratory supercomplexes from potato, Biochim. Biophys. Acta 1767 (2009) 60–67.
[30] L.A. Sazanov, P. Hinchliffe, Structure of the hydrophilic domain of respiratory complex I from *Thermus thermophilus*, Science 311 (2006) 1430–1436.
[31] U. Brandt, Proton-translocation by membrane-bound NADH: ubiquinone-oxidoreductase (complex I) through redox-gated ligand conduction, Biochim. Biophys. Acta 1318 (1997) 79–91.
[32] E.A. Baranova, P.J. Holt, L.A. Sazanov, Projection structure of the membrane domain of *Escherichia coli* respiratory complex I at 8 Å resolution, J. Mol. Biol. 366 (2007) 140–154.
[33] H. Eubel, J. Heinemeyer, H.P. Braun, Identification and characterization of respirasomes in potato mitochondria, Plant Physiol. 134 (2004) 1450–1459.
[34] F. Krause, N.H. Reifschneider, D. Vocke, H. Seelert, S. Rexroth, N.A. Dencher, "Respirasome"-like supercomplexes in green leaf mitochondria of spinach, J. Biol. Chem. 279 (2004) 48369–48375.
[35] N.V. Dudkina, J. Heinemeyer, S. Sunderhaus, E.J. Boekema, H.P. Braun, Respiratory chain supercomplexes in the plant mitochondrial membrane, Trends Plant Sci. 11 (2006) 232–240.
[36] E. Schäfer, N.A. Dencher, J. Vonck, D.N. Parcej, Three-dimensional structure of the respiratory chain supercomplex $I_1III_2IV_1$ from bovine heart mitochondria, Biochemistry 46 (2007) 2579–2585.
[37] I. Wittig, R. Carrozzo, F.M. Santorelli, H. Schägger, Supercomplexes and subcomplexes of mitochondrial oxidative phosphorylation, Biochim. Biophys. Acta 1757 (2006) 1066–1072.
[38] J.P. Abrahams, A.G. Leslie, R. Lutter, J.E. Walker, Structure at 2.8 Å resolution of F_1-ATPase from bovine heart mitochondria, Nature 370 (1994) 621–628.
[39] D. Stock, C. Gibbons, I. Arechaga, A.G. Leslie, J.E. Walker, The rotary mechanism of ATP synthase, Curr. Opin. Struct. Biol. 10 (2000) 672–679.
[40] I. Wittig, H. Schägger, Structural organization of mitochondrial ATP synthase, Biochim. Biophys. Acta 1777 (2008) 592–598.
[41] I. Arnold, K. Pfeiffer, W. Neupert, R.A. Stuart, H. Schägger, Yeast mitochondrial F_1F_0-ATP synthase exists as a dimer: identification of three dimer-specific subunits, EMBO J. 17 (1998) 7170–7178.
[42] I. Wittig, H. Schägger, Advantages and limitations of clear-native PAGE, Proteomics 5 (2005) 4338–4346.
[43] N. Buzhynskyy, P. Sens, V. Prima, J.N. Sturgis, S. Scheuring, Rows of ATP synthase dimers in native mitochondrial inner membranes, Biophys. J. 93 (2007) 2870–2876.
[44] N.V. Dudkina, G.T. Oostergetel, D. Lewejohann, H.P. Braun, E.J. Boekema, Row-like organization of ATP synthase in intact mitochondria determined by cryo-electron tomography, Biochim. Biophys. Acta. 1797 (2010) 272–277.
[45] H. Schägger, Respiratory chain supercomplexes, IUBMB Life 52 (2001) 119–128.
[46] C. Ugalde, R.J.R.J. Janssen, L.P. van den Heuvel, J.A. Smeitink, L.G.J. Nijtmans, Differences in assembly or stability of complex I and other mitochondrial OXPHOS complexes in inherited complex I deficiency, Hum. Mol. Genet. 13 (2004) 659–667.
[47] E.L. Blakely, A.L. Mitchell, N. Fisher, B. Meunier, L.G. Nijtmans, A.M. Schaefer, M.J. Jackson, D.M. Turnbull, R.W. Taylor, A mitochondrial cytochrome *b* mutation causing severe respiration chain enzyme deficiency in humans and yeast, FEBS J. 14 (2005) 3583–3592.
[48] A. Stroh, O. Anderka, K. Pfeiffer, T. Yagi, M. Finel, B. Ludwig, H. Schägger, Assembly of respiratory complexes I, III, and IV into NADH oxidase supercomplex stabilizes complex I in *Paracoccus denitrificans*, J. Biol. Chem. 279 (2004) 5000–5007.

[49] P. Paumard, J. Vaillier, B. Coulary, J. Schaeffer, V. Soubannier, D.M. Mueller, D. Brethes, J.P. di Rago, J. Velours, The ATP synthase is involved in generating mitochondrial cristae morphology, EMBO J. 21 (2002) 221–230.
[50] M.F. Giraud, P. Paumard, V. Soubannier, J. Vaillier, G. Arselin, B. Salin, J. Schaeffer, D. Brethes, P. di Rago, J. Velours, Is there a relationship between the supramolecular organization of the mitochondrial ATP synthase and the formation of cristae? Biochim. Biophys. Acta 1555 (2002) 174–180.
[51] U. Brandt, Energy converting NADH: quinone oxidoreductase (complex I), Annu. Rev. Biochem. 75 (2006) 69–92.
[52] S. Iwata, J.W. Lee, K. Okada, J.K. Lee, M. Iwata, B. Rasmussen, T.A. Link, S. Ramaswamy, B.K. Jap, Complete structure of the 11-subunit bovine mitochondrial cytochrome bc_1 complex, Science 281 (1998) 64–71.
[53] T. Tsukihara, H. Aoyama, E. Yamashita, T. Tomizaki, H. Yamaguchi, K. Shinzawa-Itoh, R. Nakashima, R. Yaono, S. Yoshikawa, The whole structure of the 13-subunit oxidized cytochrome *c* oxidase at 2.8 Å, Science 272 (1996) 1136–1144.